Iranian Journal of Astronomy and Astrophysics
Vol. 1, No. 1, 2013
© Available online at http://journals.du.ac.ir

Iranian Journal of Astronomy and Astrophysics

Evaluation of New MOND Interpolating Function with Rotation Curves of Galaxies

Hosein Haghi[1] · Hamed Ghasemi[2] · HongSheng Zhao[3]

[1] Department of Physics, Institute for Advanced Studies in Basic Sciences (IASBS), P.O. Box 11365-9161, Zanjan, Iran; email: haghi@iasbs.ac.ir
[2] Department of Physics, Zanjan University, Zanjan, Iran
[3] SUPA, School of Physics and Astronomy, University of St. Andrews, KY16 9SS, UK

Abstract. The rotation curves of a sample of 46 low- and high-surface brightness galaxies are considered in the context of Milgrom's modified dynamics (MOND) to test a new interpolating function proposed by Zhao et al. (2010) [1] and compare with the results of simple interpolating function. The predicted rotation curves are calculated from the total baryonic matter based on the B-band surface photometry, and the observed distribution of neutral hydrogen, in which the one adjustable parameter is the stellar mass-to-light ratio. The predicted rotation curves generally agree with the observed curves for both interpolating functions. We show that the fitted M/L in the B-band correlates with B-V color in the sense expected from what we know about stellar population synthesis models. Moreover, the mass-to-light ratios of MOND with new interpolating function is in consistent with scaled Salpeter's initial mass function of the SPS scheme, while those of MOND with simple interpolating function favor Kroupa IMF.

Keywords: ISM: molecules, ISM: structure, instabilities

1 Introduction

The rotation curves of spiral galaxies provide an accurate determination of the radial force distribution in spiral galaxies. They are the major observational basis of understanding disparity between the visible mass and the classical dynamical mass in large astronomical systems. There are two explanations for this problem; assuming a large quantities of unseen matter (dark matter) along with these systems or changing the Newtonian gravity law on large scales.

Despite more than 30 years of intense effort, no candidate particles of dark matter have yet been directly detected, no annihilation radiation from it, no evidence from reactor experiments supporting the physics (beyond the standard model) upon which dark matter candidates are based. Therefore, the impression of modifying the standard gravitational theories on large scales has been progressed in recent years.

Some alternatives to the Newtonian dynamics have been proposed. Modified Newtonian Dynamics (MOND; Milgrom 1983)is one of the earliest of such theories that could explain the flat rotation curves [2, 3, 4, 5] with considerable success. Also it could explain the Tully-Fisher relation (the observed correlation between the asymptotic rotation speed and the total baryonic mass of galaxies as $V_\infty^4 \propto M$ which is not well understood in the context of dark matter) with considerable success [6]. The MONDian dynamics can also explain the standard hieratical bottom-up scenario of structure formation in the universe [7, 8]. Although, MOND is very successful in galactic scales, it faces numerous challenges. MOND

theory can not explain the internal dynamics of galaxy clusters and the merging of clusters of galaxies, without the introduction of dark matter [9, 10]. Recently Haghi et al (2009) [11] and Jordi et al (2009)[12] have shown that the MOND also can not justify the internal dynamics of some galactic globular clusters.

Within the MOND framework, the gravity (or inertia) does not follow the prediction of Newtonian dynamics for acceleration smaller than $a_0 = 1.2 \times 10^{-10} ms^{-2}$, as derived from galaxy rotation curves fit. For a galaxy with a density distribution ρ, the acceleration of stars satisfies the modified Poisson equation

$$\nabla.[\mu(\frac{\nabla\Phi}{a_0})\nabla\Phi] = 4\pi G\rho, \tag{1}$$

where $\mu(x)$ is some interpolating function with the property that $\mu(x) = x$ at $x \ll 1$ to $\mu(x) = 1$ at $x \gg 1$. Because this can be derived from a Lagrangian, it ensures conservation of energy, momentum, and angular momentum [13]. In brief, for symmetric mass distribution, the MONDian acceleration, g related to Newtonian acceleration g_N through the following relation:

$$g\mu(\frac{g}{a_0}) = g_N, \tag{2}$$

There are several suggestions for the functional form of interpolating function. However, while the precise functional form of the interpolating function is not necessary to make many fundamental predictions [4], it is nevertheless important in order to fit the rotation curves of galaxies. Among those three functions commonly used in different systems. The standard interpolating function as

$$\mu_1(x) = \frac{x}{\sqrt{1+x^2}}, \tag{3}$$

was originally put in by hand, and does not derive from any physical principle. However, with the number of galaxies with good data increasing, the freedom of this function should be restrained by the observations. Famaey & Binney (2005)[14] , have found the simple interpolating function,

$$\mu_2(x) = \frac{x}{1+x}, \tag{4}$$

gives a better fit to the terminal velocity curve of the Milky Way, while yielding an extremely good fit to the rotation curve of the standard external galaxy NGC3198.

The toy free function in the scalar action of Bekenstein (2004) [15] gives rise to the following interpolating function

$$\mu_3(x) = \frac{\sqrt{1+4x}-1}{\sqrt{1+4x}+1}, \tag{5}$$

The simple function is compatible with the relativistic theory of MOND (TeVeS) that was put forward by Bekenstein (2004)[15]. The typical value for the parameter a_0, obtained from analysis of a sample of spiral galaxies with high-quality rotation curves is $a_0 = 1.2 \pm 0.27 \times 10^{-10} ms^{-2}$ [2]. Famaey et al. (2007)[16] showed that using simple function leads to a slightly different value of $a_0 = 1.35 \times 10^{-10} ms^{-2}$.

This simply shows the variety of shapes that the interpolating function of MOND can take in principle. Very precise data for rotation curves, including negligible errors on the distance and on the stellar mass-to-light ratios (or, in that case, purely gaseous galaxies) should allow one to pin down its precise form, at least in the intermediate gravity regime.

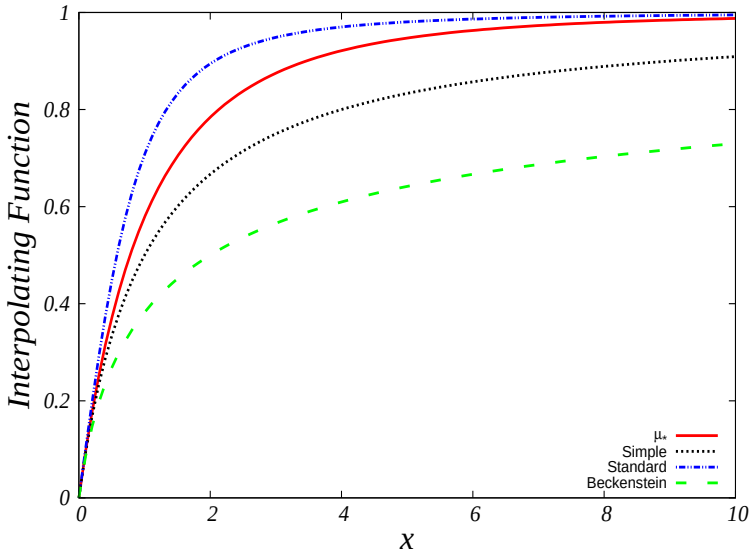

Figure 1: Various μ-functions. The Dotted black line and dashed-dotted line correspond to the simple and standard interpolating function, respectively. The short-dashed line is the interpolating function explored by Bekenstein (2004)[15]. The red solid line indicates the μ_*-function defined in Eq. 6. The latter function

Recently, a new interpolating function considered in the literature, suggested by Zhao et al. (2010)[1], in the form of

$$\mu_*(x) = 1 - \frac{1}{(1+\frac{x}{3})^3}. \tag{6}$$

Since one of the most striking successes of MOND is the ability of Milgroms formula to fit the rotation curves of a wide range of galaxies. In this paper we constructed rotation curves of a large sample of galaxies from the distribution of their detectable matter in the context of MOND to evaluate the new proposed interpolating function, $\mu_*(x)$, and compare the results of simple function, $\mu_2(x)$.

Figure 1 shows how fast the various μ-function transit between newotonian regime and MOND regime. Among these functions the standard function raises more quickly than others and Bekenstein interpolating function triggers too slow a transition from the MONDian to the Newtonian regime.

The plane of the paper is as follow. In section 2 the data on the rotation curve is presented. The fitting procedure is carried out in section 3. The results of the fit are presented in section 4.

2 The Data

In order to test the new interpolating function, we have therefore considered a sample of 46 galaxies taken from Sanders (1996)[3], McGaugh & de Blok (1998)[17], Sanders & Verheijen (1998)[7] and Begeman (1991)[2], accommodates these diversities. The sample contains several high surface brightness (HSB), massive stellar component, and low gas content as

well as a number of dwarf, gas-dominated and low surface brightness (LSB) galaxies. They are listed in Table 1 and shown in Figs. 2 - 4.It is generally believed that deviations from the classical dynamics is more pronounced in LSBs than in HSBs. ([17, 18, 19]). Twenty-eight members of the sample, of both HSB and LSB types, are located in the Ursa Major cluster of galaxies, believed to be at the distance of about 15.5 Mpc ([20]). Seven of the galaxies, listed in Table 3, have central bulges and are treated differently, to be explained shortly. For a full description of the sample the interested reader is referred to Sanders and McGaugh (2002)[4].

3 Fitting the Rotation Curves

In order to calculate MOND rotation curves, the first step is to determine the Newtonian acceleration of the detectable matter, g_N via the classical Poisson equation. Given the Newtonian acceleration, the effective acceleration is calculated from the MOND formulae (2). For the interpolating function $\mu_2(x)$ we can obtain $\mathbf{g}$ in terms of $\mathbf{g_N}$ as follow:

$$\mathbf{g} = \mathbf{g}_N \left[\frac{1}{2} + \frac{1}{2}\sqrt{1 + (\frac{4a_0}{g_N})}\right]. \tag{7}$$

Therefore, rotation curves in this model calculated as follow:

$$v^2_{Mond} = \frac{GM}{r}\left(\frac{1 + \sqrt{1 + \frac{4a_0 r^2}{GM}}}{2}\right), \tag{8}$$

where $M = M_{stars} + M_{bulge} + M_{gas}$, M_{stars}, M_{bulge}, and M_{gas} are the total baryonic, stellar disk, bulge, and gaseous disk, respectively. The amplitude of M_{stars} and M_{bulge} which are determined by photometric observations can be scaled according to the chosen, or fitted, stellar mass-to-light (M/L) ratio. The value of M_{gas} is derived from HI observations, when they are available.

We assume a constant M/L ratio, throughout the galaxy, though this is not strictly the case, because of the color gradient in spiral galaxies. However, in seven bulged spirals we find assigning different M/L to the bulge and the disk improves fittings to the observed data. We assume the HI gas is in co-planer rotation about the center of the galaxy, an assumption which may not hold in galaxies with strong bars ([4]).

If eq. 6 is chosen as the interpolation function instead of eq. 4, the equivalent of eq. 8 becomes as a forth order polynomial equation:

$$v^4_{Mond} + r(9a_0 - g_N)v^3_{Mond} + r^2(27a_0^2 - 9a_0 g_N)v^2_{Mond} - 27a_0^2 g_N r^3 v_{Mond} - 27a_0^3 g_N r^4 = 0 \tag{9}$$

In order to solve this equation we used the Horner algorithem. Given the observed distribution of the baryonic matter (stellar and gaseous disks, plus a spheroidal bulge, if present), the circular speed, is calculated from Eqs. (8) and (9).

To fit the observational velocity curve with the theoretical model we employ the χ^2 goodness-of-fit test, that tell us how close are the theoretical to the observed values. Fitting of the calculated rotation curves to the observed data points is achieved by adjusting the M/L ratio, through a least-square χ^2, defined as

$$\chi^2 = \frac{1}{(N - P - 1)}\sum_{i=1}^{N}\frac{(v^i_{Mond} - v^i_{obs})^2}{\sigma_i^2}, \tag{10}$$

where σ_i is the observational uncertainty in the rotation speeds and P is the number of degrees of freedom. The M/L ratio of the disk and of the bulge are our ultimate results.

4 Results

In figures 2 - 4 we show the results of the fits of theoretically constructed rotation curves to the observations of 46 galaxies.

4.1 μ_* versus μ_2

In figure 5 we plot the minimum χ^2 achievable for all galaxies, using two different interpolating functions. Each galaxy in figure 5 has two different values for minimum χ^2; the black and red columns correspond to the results of MOND fit to rotation curve assuming μ_* and the simple function μ_2, respectively.

Overall, MOND gives good fits to the rotation curves of these systems for both interpolating function without invoking any dark contents. In particular, with only one free parameter, MOND can explain well the observed kinematics. The best-fit χ^2 and M/L values for two interpolating functions are listed in Table 1. As can be seen, in average, a lower χ^2 can be achieved by using μ_*. For example for the specific cases of NGC 6446, DDO 168, NGC 2998, NGC 6946, NGC 2885, the minimum χ^2s are decreased by a factor of ~ 0.7.

4.2 Compliance with SPS Models

In this section we compare the mass-to-light ratios obtained from MOND rotation curve fits with the independent expectations of stellar population synthesis models.

In Bell & de Jong (2001) [21] they showed that stellar population synthesis (SPS) models predict a tight linear relation between the color and mass-to-light ratio of a stellar population. Redder galaxies should have larger M/L (see, e.g., [21, 22, 23]). The normalization of this relation depends critically on the shape of the stellar IMF at the low-mass end. These faint stars contribute significantly to the mass, but insignificantly to the luminosity and color of a stellar system [21]. The slope of this linear relation does not depend on exact details of the history of star formation, i.e. the assumed IMF. Bell et al. (2003)[22] suggested the color-M/L relation using scaled Salpeter IMF as

$$\log(M/L_B) = 1.74(B-V) - 0.94. \tag{11}$$

There are other IMF's leading to slightly different relations. Kroupa (2001)[24], introduces a turnover at the low mass end of his IMF. The slope 1.74 is insensitive to such variations in IMF, but the y-intercept is. To obtain the equivalent relation for Kroupa's IMF one should shift Eq. (11) and the plots in Figure (6) down by roughly (-0.35) dex, ([22]).

In Figure 6, we contrast M/L ratios of MOND using two interpolating functions against the predictions of SPS. The solid line is the best fit to the data points obtained from the analysis of the rotation curves. The theoretical SPS predictions of [21], and [22], for different IMFs are also plotted. The slope of MOND with simple function is 1.88, of MOND with μ_*-function is 1.87 ± 0.23. The slope for both function are consistent with SPS predictions. The corresponding y-intercepts, -1.15, and -1.03, respectively, are also in harmony with that of scaled Salpeter IMF and Kroupa IMF and .

The obtained M/L ratios for both μ-function fulfill this expectation, albeit with different IMFs. This is noteworthy, as there is no explicit/implicit connection between the basic tenets of the SPS and MOND.

5 Conclusion

Rotation curves of spiral galaxies, as observed in the 21 cm line of neutral hydrogen, are a useful tool to determine the radial force distribution very low gravitational acceleration regime. MOND as an alternative theory for dark matter hypothesis, has been tested by means of rotation curve analysis using several galaxy samples and various interpolating functions. Recently, Zhao et al (2010) [1] proposed a new interpolating function that works well in cosmological scales. In this paper we used the new function of MOND to deduce the dynamics of a good size sample of high and low surface brightness galaxy types, and check the results against observations.

Rotation curves are constructed with only one free adjustable parameter, the stellar mass-to-light ratio. We obtain the mass to light ratios of the galaxies, via best fit analysis by considering the new interpolating function and compare the results with simple interpolating function. We found that, the predicted rotation curves based on the new proposed μ-function are compatible with observed curves. Using μ_* function, in 24 galaxies, the minimum are lower than those obtained using simple function. Therefore, we conclude that the new interpolating function can fits rotation curves as well as simple function.

In addition, we examine the correlation between color and inferred mass to light ratios. Stellar population synthesis models impose constrains on stellar M/L: Redder galaxies should have larger M/L ratios. SPS predictions of M/L ratios are sensitive to the adopted IMF. For example, as shown in figure 6, the M/L ratios inferred from Salpeter's IMF are notably larger than those obtained from Kroupa's.

Using μ_* function, the range of inferred M/L ratios is generally reasonable and is consistent with population synthesis models. The best-fit values of stellar mass-to-light ratios, obtained on purely dynamical grounds assuming MOND, vary with galaxy color as one would expect on purely astrophysical grounds from stellar population synthesis models. There is absolutely nothing built into MOND that would require that redder galaxies should have higher stellar mass-to-light ratios, but this is what the rotation curve fits require.

Although these different μ-functions yields fairly similar rotation curves in galaxies, their predictions in the solar system differ greatly. For μ_* function, the solar system experiences an non-$1/r^2$ force, $g_{non} = (1-\mu)g = [1+g/(3a_0)]^{-3}g \approx 27[(GM_\odot)/(r^2a_0)]^{-2}a_0 = 10^{-6}a_0(r/100AU)^4$, which is much smaller compared to the standard μ-function predicted extra force of $\approx [(GM_\odot)/(r^2a_0)]^{-1}a_0/2 = 10^{-4}a_0(r/100AU)^2$, and even smaller than the simple μ-function predicted $\sim a_0$ extra force. The precession speed of the planets prefers models like μ_* and the standard, but the simple μ-function (if without modification) predicts too much extra force [1, 25, 26]. In a future contribution we will also discuss the the solar system differences of the two μ_* and simple functions.

Table 1: Properties of sample galaxies, and the best-fit values of stellar M/L from minimizing χ^2. Upper part and lower part show 32 HSB and 14 LSB galaxies, respectively. Explanation of the columns: name of the galaxy; color; the best fit stellar M/L ratio and corresponding χ^2 for MOND model using interpolating function Eq. 6. The last two columns are the results for model using simple interpolating function (Eq. 4) in Hubble types are from NASA/IPAC Extragalactic Database (NED). Bulged galaxies are marked by a superscript '^{b}'.

Galaxy (Type)	B-V	$(M/L)_*$	χ^2_*	$(M/L)_{simple}$	χ^2_{simple}
M 33 (Sc)	0.55	0.5	24.72	0.4	28.13
NGC 300 (Sc)	0.58	0.6	2.47	0.5	2.17
NGC 2903 (Sc)	0.55	2.5	7.66	2	7.81
NGC 3726 (SBc)	0.45	0.8	4.52	0.6	5.18
NGC 3769 (SBb)	0.64	1	0.71	0.8	0.7
NGC 3877 (Sc)	0.68	1.4	3.14	1.1	3.19
NGC 3893 (Sc)	0.56	1.3	2.9	1.1	2.36
NGC 3949 (Sbc)	0.39	0.7	5.52	0.6	4.87
NGC 3953 (SBbc)	0.71	2.4	0.73	1.9	0.56
NGC 3972 (Sbc)	0.55	1.2	3.54	0.9	3.48
NGC 3992 (SBbc)	0.72	4.2	1.08	3.3	1.29
NGC 4013 (sb)	0.83	2.6	1.57	2.1	1.57
NGC 4051 (SBbc)	0.62	1	0.92	0.8	0.91
NGC 4085 (Sc)	0.47	0.8	8.3	0.7	8.14
NGC 4088 (Sbc)	0.51	0.9	1.89	0.7	2.06
NGC 4100 (Sbc)	0.63	2	2.06	1.6	2.03
NGC 4138 (Sa)	-	3.1	1.66	2.5	1.38
NGC 4157 (Sb)	0.66	2	0.97	1.6	1.00
NGC 4217 (Sb)	0.77	1.9	3.33	1.5	3.03
NGC 4389 (SBbc)	-	0.3	8.1	0.3	8.04
NGC 5585 (SBcd)	0.46	0.4	11.43	0.3	11.14
NGC 6946 (SABcd)	0.40	0.4	14.68	0.3	20.02
NGC 7793 (Scd)	0.63	1	1.61	0.8	1.65
UGC 6399 (Sm)	-	0.8	0.22	0.7	0.20
UGC 6973 (Sab)	-	2.4	17.06	2.1	13.12
NGC 801^b (Sc)	0.61	0.9	19.34	0.8	16.36
NGC 2998^b (SBc)	0.45	1	2.92	0.8	4.32
NGC 5371^b (S(B)b)	0.65	1.4	11.3	1.1	11.65
NGC 5533^b (Sab)	0.77	2.8	2.52	2.2	2.67
NGC 5907^b (Sc)	0.78	3.4	4.67	2.7	5.62
NGC 6674^b (SBb)	0.57	2.3	10.6	1.9	11.28
UGC 2885^b (Sbc)	0.47	1.3	3.14	1.1	4.00
DDO 168 (SO)	0.32	0.1	15.83	0.1	19.26
NGC 247 (SBc)	0.54	0.9	4.08	0.7	4.11
NGC 1560 (Sd)	0.57	0.8	2.51	0.4	1.65
NGC 3917 (Scd)	0.60	1.1	5.09	0.9	5.28
NGC 4010 (SBd)	0.54	1.1	2.12	0.9	1.94
NGC 4183 (Sa)	0.39	0.6	1.07	0.4	1.56
UGC 128 (Sdm)	0.60	0.9	0.62	0.7	0.81
UGC 6446 (Sd)	0.39	0.5	3.29	0.3	4.76
UGC 6667 (Scd)	0.65	0.9	1.11	0.7	1.04
UGC 6917 (SBd)	0.53	1.2	0.83	0.9	0.87
UGC 6923 (Sdm)	-	0.6	1.73	0.5	1.51
UGC 6930 (SBd)	0.59	0.7	0.38	0.5	0.57
UGC 6983 (SBcd)	0.45	1.4	1.56	1.1	1.88
UGC 7089 (Sdm)	-	0.2	0.25	0.1	0.35

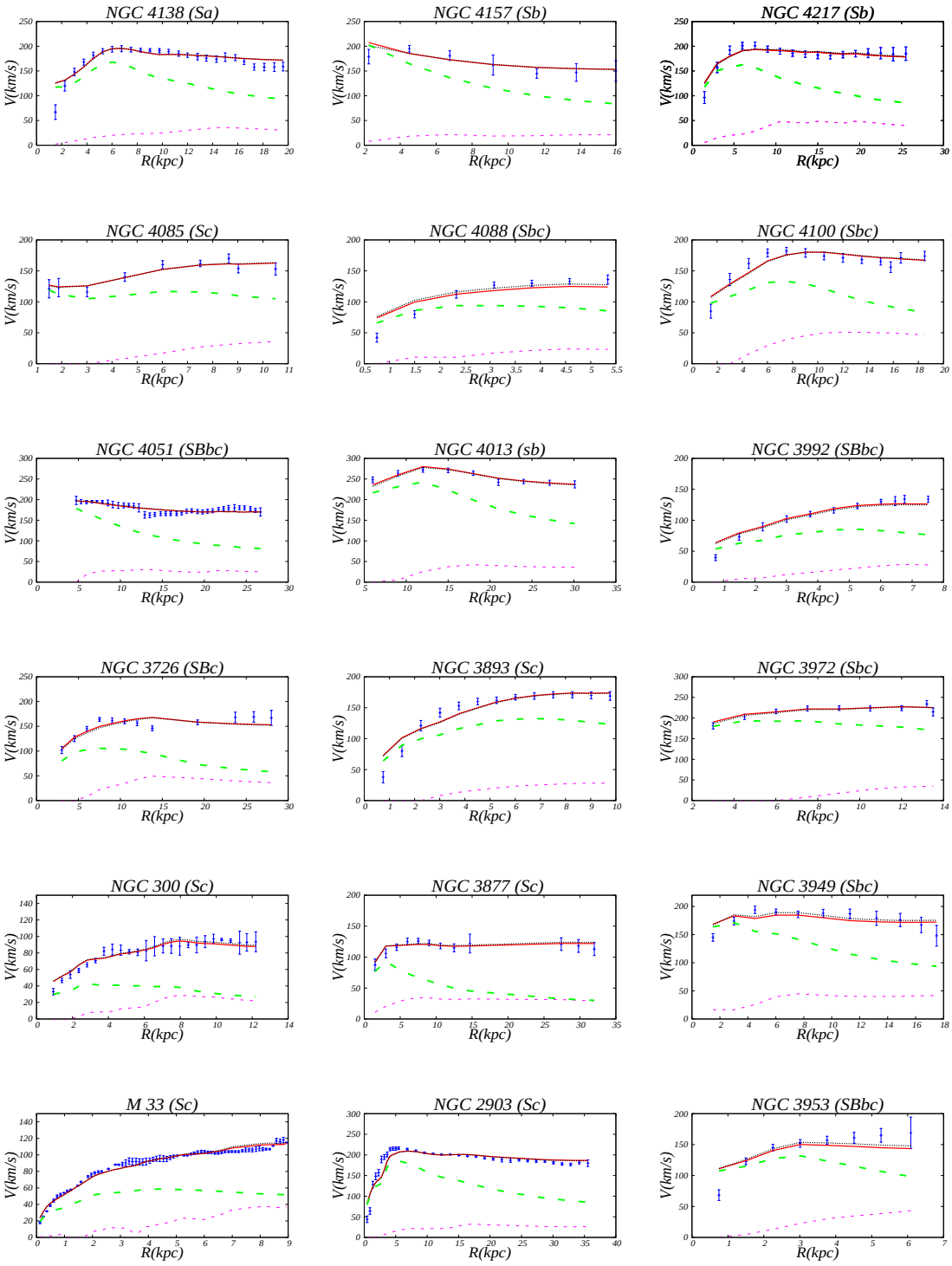

Figure 2: Best fit rotation curves superimposed to the observed data (points with vertical error bars) for the sample of 46 HSB and LSB galaxies. See Table 1 for details on the galaxies and the values of the best fit parameters. Short and long dashed lines are contributions of the gaseous and stellar components to the Newtonian rotation speeds, respectively. M/Ls of Mond with simple function are used in plotting the stellar component. Solid red line is the rotation curve constructed through MOND model with interpolating function μ_*. Black dotted line is that of MOND with simple function.

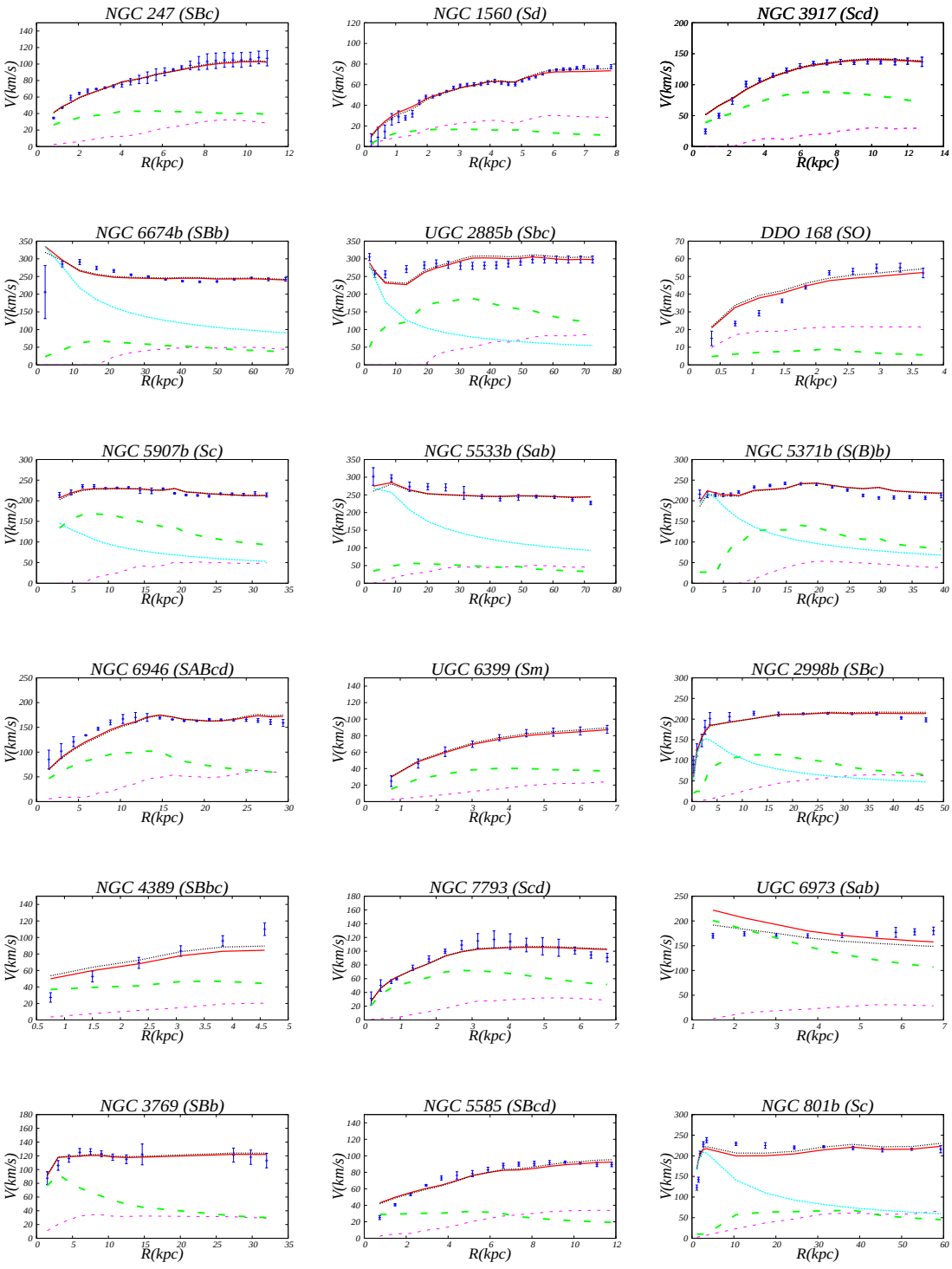

Figure 3: Fig. 2 continued.

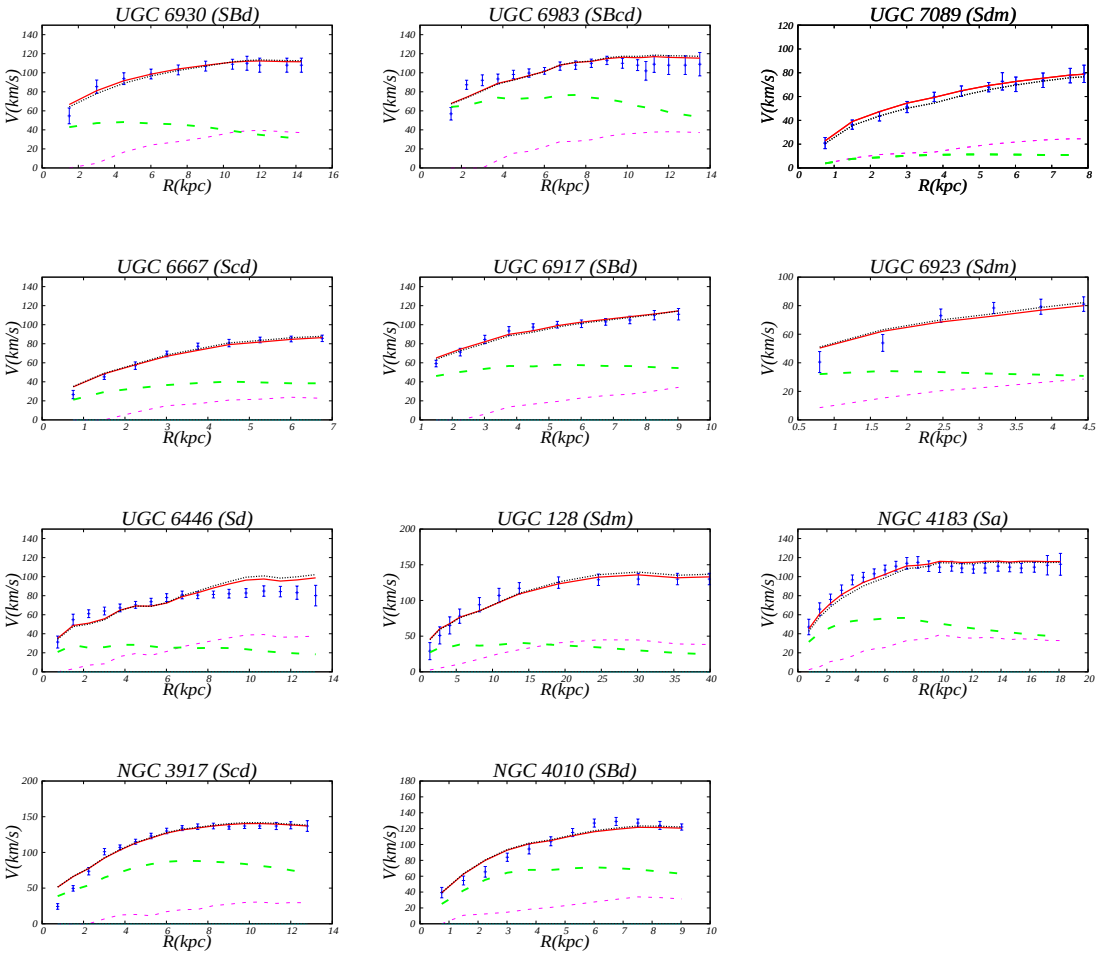

Figure 4: Fig. 2 continued.

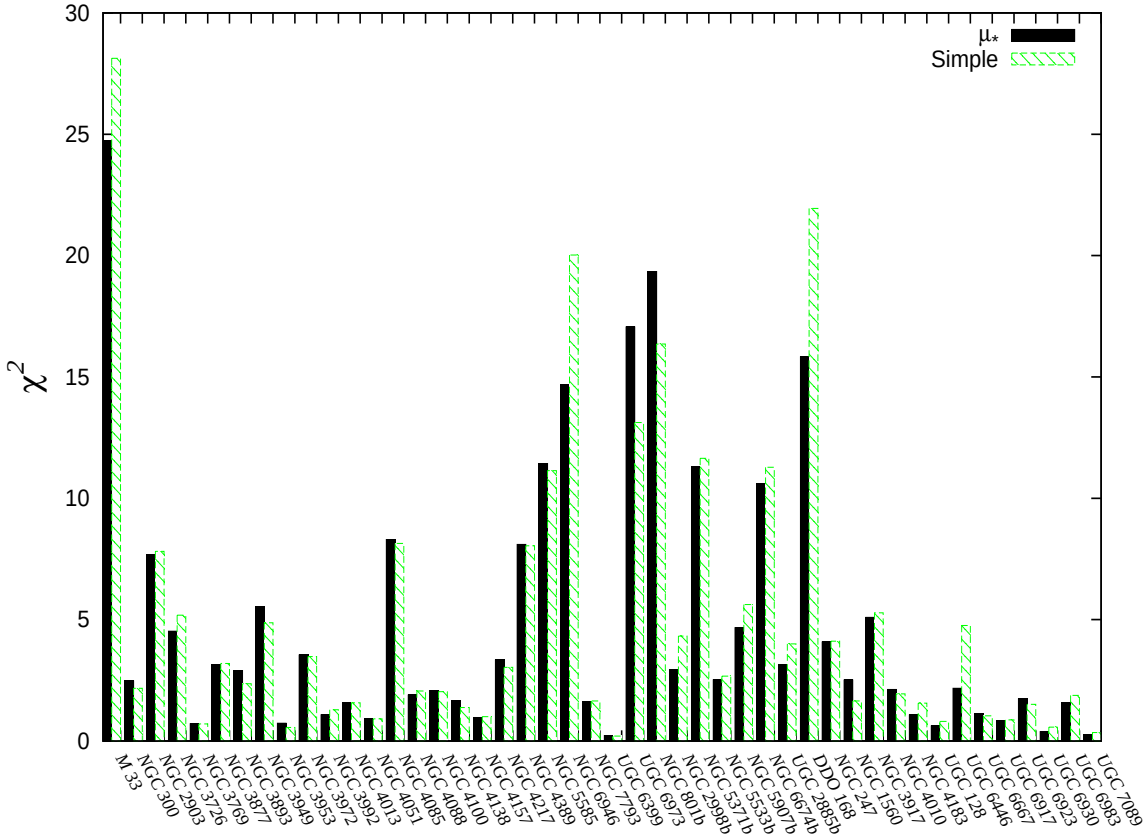

Figure 5: Comparison of minimum χ^2 values for the best fit model various μ-functions, Eq. 6 and Eq. 4.Overall, we can see that the values of χ^2 for MOND with simple function is larger than with μ_*.

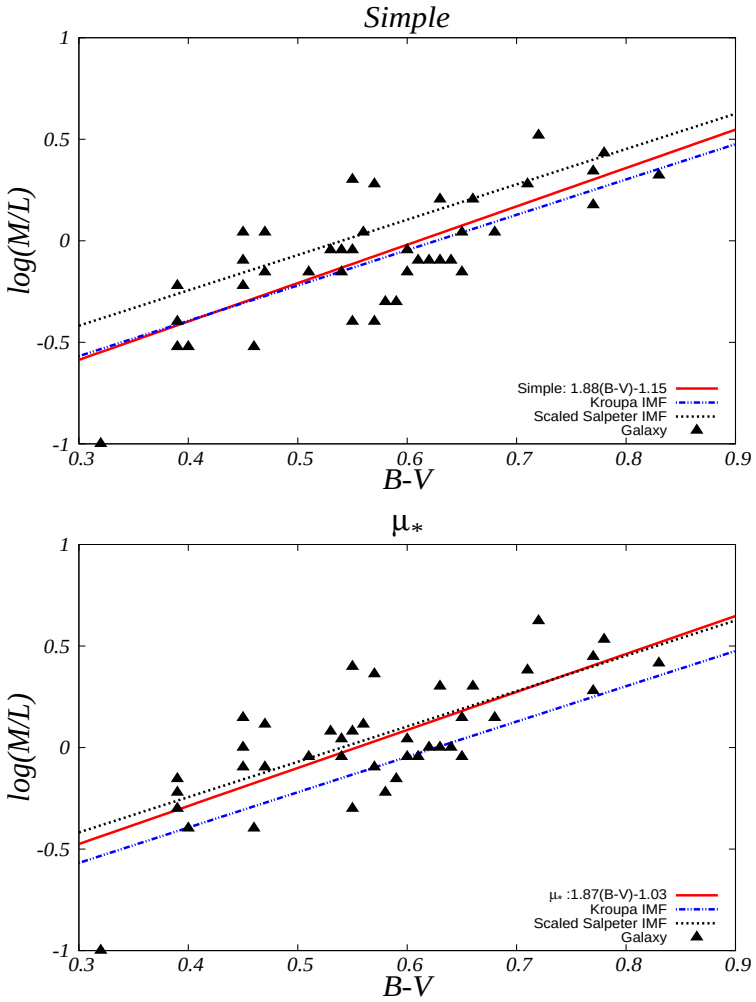

Figure 6: A comparison of the stellar M/L ratios obtained from MOND rotation curve fits (points) with the independent expectations of stellar population synthesis models (lines). Plots of stellar M/L ratios versus color, $B-V$. The data points in upper and lower panels are the best fit stellar M/L ratios has been obtained for MOND with interpolating function μ_2 and μ_*, respectively . Solid line in each panel is the best fitted line to the data points. Slopes and y-intercepts of best-fitted lines are shown in the panels. Other lines denote the theoretical predictions of SPS with different IMFs ([21, 22]). They have almost the same slope but different y-intercepts. Slopes of MOND with both interpolating functions are reasonably close to the prediction of SPS.

References

[1] Zhao H. S., Li Boojin., Beinayme O. PRD, vol 82 p 10

[2] Begeman K. G., Broeils A. H., Sanders R. H., 1991, MNRAS, 249, 523

[3] Sanders R. H., 1996, ApJ, 473, 117

[4] Sanders R. H., McGaugh S. S., 2002, ARA&A, 40, 263

[5] Famaey B., McGaugh S., 2012, Living Rev. Relativity, 15, 10

[6] McGaugh S. S., Schombert J. M., Bothun G. D., de Blok W. J. G., 2000, ApJ, 533, L99L102 .

[7] Sanders R. H., Verheijen M. A. W., 1998, ApJ, 503, 97-108

[8] Malekjani M., Rahvar S., Haghi H., 2009, ApJ, 694 : 1220-1227

[9] Clowe D., *et al.*, 2006, ApJ, 648, L109

[10] Angus G. W., Famaey B., Zhao H. S., 2006, MNRAS, 371, 138

[11] Haghi H., Baumgardt H., Kroupa P., Grebel E . K., Hilker M., Jordi K., 2009, MNRAS, 395, 1549

[12] Jordi K., Grebel E. K., Hilker M., Baumgardt H., Frank M., Kroupa P., Haghi , H., Cote P., Djorgovski S . G., 2009, AJ , 137, 4586

[13] Bekenstein J. D., Milgrom M., 1984, ApJ, 286, 7

[14] Famaey B., Binney J., 2005, MNRAS, 363, 603

[15] Bekenstein J. D., 2004, Phys. Rev. D, 70, 083509

[16] Famaey B., Bruneton J. P., Zhao H., 2007, MNRAS, 377L, 79F

[17] McGaugh S. S., de Blok W. J. G., 1998, ApJ, 499 : 41-65

[18] Sanders R. H., Noordermeer E., 2007, MNRAS, 379, 702

[19] Gentile G., Baes M., Famaey B., Van Acoleyen K., 2010, arxiv:1004.3421

[20] Tully R. B., Verheijen M. A. W., 1997, ApJ, 484, 145

[21] Bell E. F., de Jong R. S., 2001, ApJ, 550, 212

[22] Bell E. F., McIntosh D. H., Katz N., Weinberg M. D., 2003, ApJS, 149, 289

[23] Portinari L., Sommer-Larsen J., and Tantalo R., 2004, MNRAS, 347, 691

[24] Kroupa P., 2001, MNRAS, 322, 231K

[25] Galianni P., Feix M., Zhao H. S., Horne K., 2012, Phys. Rev. D., 86, 044002

[26] Sereno M., Jetzer Ph., 2006, MNRAS, 371, 626

[27] Sanders R. H., 1998, MNRAS, 296, 1009

[28] Tully R. B., Fisher J. R., 1977, A&A, 54, 661

[29] Gentile G., 2008, ApJ, 684, 1018

[30] McGaugh S. S., de Blok W. J. G., 1998, ApJ, 499 : 66-81

[31] McGaugh S. S., 2005, ApJ, 632, 859

[32] Milgrom M., 1983, ApJ, 270, 365

[33] Noordermeer E., 2008, MNRAS, 385, 1359

[34] Salpeter E. E., 1955, ApJ, 121, 161

[35] Salucci P., Lapi A., Tonini C., Gentile G., Yegorova I., Klein U., 2007, MNRAS, 378, 41